

Quasi-atomic behaviour of nanocrystals in superlattices

Variation of optical properties and structure of caesium lead halide perovskite nanoparticles in a supercrystal

Advances of the self-assembly of colloidal nanocrystals (NCs) from solution into three-dimensional arrays with long-range order have enabled the design of microscopic supercrystals that approach the structural precision of atomic single crystals [1]. As the building blocks of a supercrystal, the individual NCs are often regarded as 'artificial atoms'. A large structural coherence of these supercrystals facilitates new collective optoelectronic properties, which makes them prospective materials for electronics and photovoltaics. However, a critical question remains: whether this artificial atom analogy can also be transferred to the corresponding optical properties of NC supercrystals?

To answer the question on these metamaterials and their unique optical properties [2-4], we studied self-assembled supercrystals consisting of perovskite nanocrystals with two different chemical compositions: CsPbBr₂Cl and CsPbBr₃. The NCs are monodisperse cubes with a diameter of 7 nm for CsPbBr₂Cl and 9 nm for CsPbBr₃. Spatially

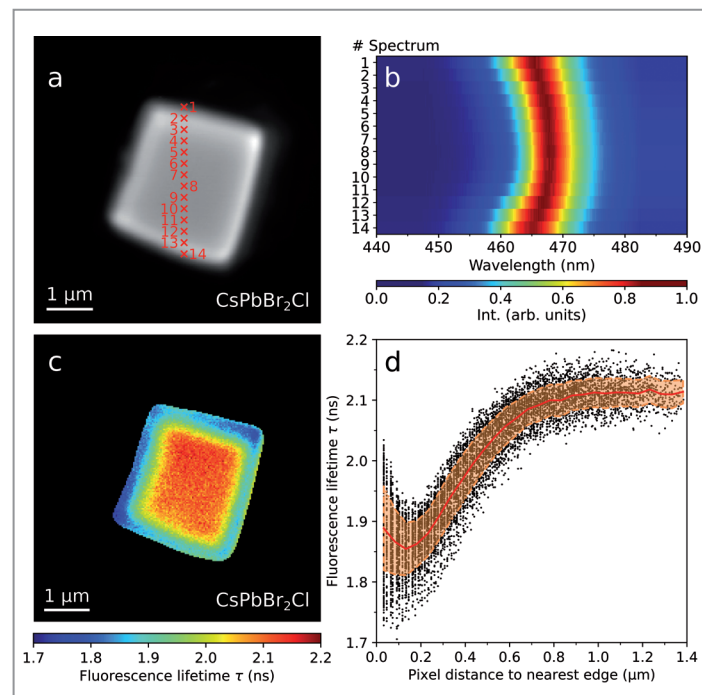


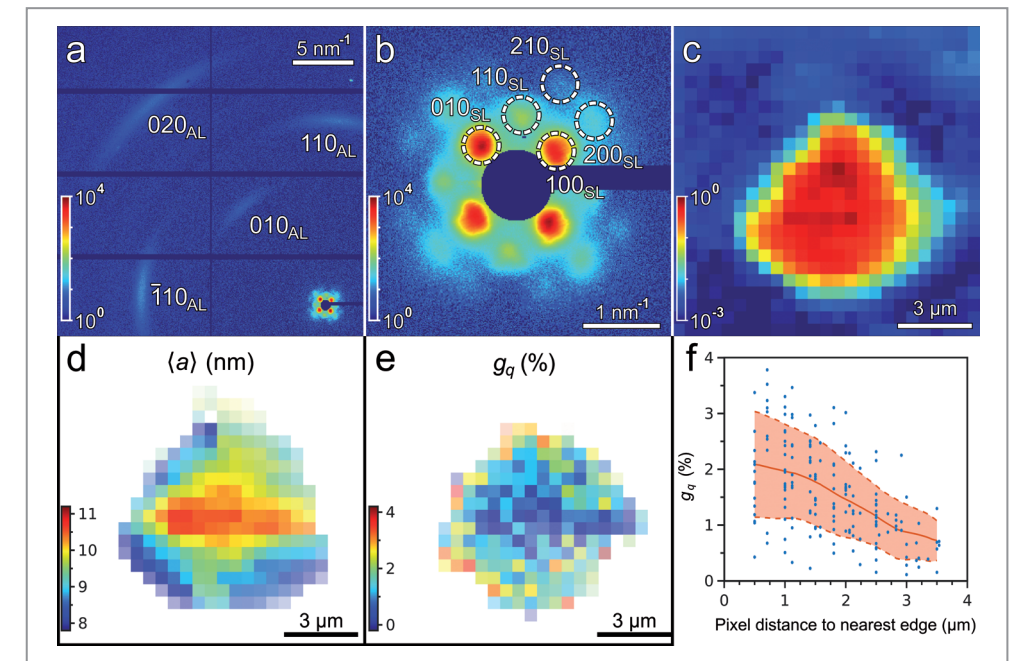
Figure 1 Spatially resolved fluorescence and lifetime imaging. a) Optical micrograph of a CsPbBr₂Cl NC supercrystal. b) The corresponding normalized spectra. c) Fluorescence lifetime τ map of a CsPbBr₂Cl NC supercrystal. d) Fluorescence lifetime values τ obtained at each pixel inside the supercrystal as a function of the distance to the nearest edge. (Adapted from a figure in the original publication licensed under CC BY 4.0.)

resolved photoluminescence spectra of the 2.5 μm thick CsPbBr₂Cl NC supercrystal samples on glass substrate under 405 nm excitation in a confocal laser scanning microscope are shown in Fig. 1 (a,b). When approaching an edge of the supercrystal, a continuous blueshift of the emission peak wavelength takes place. This blueshift is strongest for relatively small and highly faceted supercrystals, where it reaches energies up to 20 meV. In the case of supercrystals composed of CsPbBr₂Cl NCs, we measure typical fluorescence lifetimes (τ) around 2.1 ns in the centre which decrease by approximately 20% when scanning from the centre of a supercrystal towards its edges (see Fig. 1 (c,d)).

To find out the origin of these differences in the fluorescence spectra, which change from the centre of the supercrystal to its edges, we investigated its structure and carried out a synchrotron X-ray diffraction experiment at the PETRA III beamline P10. Using an X-ray beam focused to approximately 400 nm \times 400 nm on the sample, we performed a spatially resolved scan of a typical CsPbBr₂Cl NC supercrystal on a Kapton substrate. The averaged wide-angle X-ray scattering pattern (WAXS) is shown in Fig. 2a. The small-angle X-ray scattering (SAXS) region (Fig. 2b) displays several orders of Bragg peaks, corresponding to a simple cubic structure. A real space map of the scan based on the integrated SAXS intensity, corresponding to a single supercrystal is shown in Fig. 2c. Analysing individual SAXS patterns from different locations on the supercrystal, we find that the lattice parameter decreases from the value of $a = 10.7$ nm in the centre of the supercrystal down to $a = 7.8$ nm at the edges (Fig. 2d).

Despite the fact that the atomic average lattice parameter of the NCs a_{AL} is constant throughout the whole supercrystal,

Figure 2 Spatially resolved X-ray nanodiffraction experiment performed on a CsPbBr₂Cl NC supercrystal: a) Average diffraction pattern for a supercrystal. b) Enlarged SAXS region of the averaged diffraction pattern. c) Diffraction map for a scan based on the integrated intensity of the SAXS diffraction patterns at $q < 2$ nm⁻¹. d) Spatially resolved SAXS. An extracted average unit parameter $\langle a \rangle$ is shown. e) Atomic lattice distortion g_q extracted from the Williamson-Hall method. f) The same value g_q for each pixel plotted against the distance from this pixel to the nearest edge of the supercrystal. (Adapted from a figure in the original publication licensed under CC BY 4.0.)



we find a difference in the radial width of the WAXS Bragg peaks at different locations. By the Williamson-Hall method, we extract the atomic lattice distortion $g_q = \delta a_{\text{AL}} / a_{\text{AL}}$ at each spatial point. We find a clear trend of increasing atomic lattice distortion towards the edges of the supercrystal with a maximum of 2% at the edge, as shown in Fig. 2 (e,f). This indicates that, during the process of self-assembly into supercrystals from colloidal solution by slow drying, not only the superlattice exhibits distortions at the edges of supercrystal [5], but also the individual NCs are highly strained at the edges.

To rationalise the experimental trend of increased fluorescence energies at the edges of the supercrystal as compared to its centre, we carried out density functional modeling of the system. Overall, our computational modeling suggests that the spectral blueshift of the fluorescence from the edges of the supercrystal can be caused mainly due to a reduced NC coordination number at the edges as well as the compressive atomic lattice strain.

In conclusion, supercrystals of lead halide perovskite NCs self-assembled from solution exhibit a loss in structural coherence, an increasing atomic misalignment between adjacent NCs and compressive strain near their surfaces. These structural distortions are strongly correlated with a blueshifted fluorescence and decreased radiative lifetimes. Our results emphasise the importance of minimising strain during the self-assembly of perovskite nanocrystals into supercrystals for photovoltaic applications such as superfluorescent emitters. The correlations between structure and fluorescence in supercrystals revealed here are thus another example for the analogy between atoms and NCs as so-called quasi-atoms.

Author contact:

Marcus Scheele, marcus.scheele@uni-tuebingen.de
Ivan Vartanyants, ivan.vartanyants@desy.de

References

1. S. Toso et al., 'Multilayer diffraction reveals that colloidal superlattices approach the structural perfection of single crystals', *ACS Nano* 15, 6243–6256 (2021).
2. G. Rainò et al., 'Superfluorescence from lead halide perovskite quantum dot superlattices', *Nature* 563, 671–675 (2018).
3. Y. Tong et al., 'Spontaneous self-assembly of perovskite nanocrystals into electronically coupled supercrystals: toward filling the green gap', *Adv. Mater.* 30, 1801117 (2018).
4. I. Cherniukh et al., 'Perovskite-type superlattices from lead halide perovskite nanocubes', *Nature* 593, 535–542 (2021).
5. N. Mukharamova et al., 'Revealing grain boundaries and defect formation in nanocrystal superlattices by nanodiffraction', *Small* 15, 1904954 (2019).

Original publication

'Spatially resolved fluorescence of caesium lead halide perovskite supercrystals reveals quasi-atomic behavior of nanocrystals', *Nature Communications* 13, 892 (2022). DOI: 10.1038/s41467-022-28486-3



Dmitry Lapkin¹, Christopher Kirsch², Jonas Hiller², Denis Andrienko³, Dameli Assalauova⁴, Kai Braun², Jerome Carnis⁵, Young Yong Kim¹, Mukunda Mandal³, Andre Maier^{2,4}, Alfred J. Meixner^{2,4}, Nastasia Mukharamova⁴, Marcus Scheele^{2,4}, Frank Schreiber^{4,5}, Michael Sprung¹, Jan Wahl², Sophia Westendorf², Ivan A. Zaluzhnyy⁵ and Ivan A. Vartanyants¹

1. Deutsches Elektronen-Synchrotron DESY, Hamburg, Germany
2. Institut für Physikalische und Theoretische Chemie, Universität Tübingen, Tübingen, Germany
3. Max Planck Institute for Polymer Research, Mainz, Germany
4. Center for Light-Matter Interaction, Sensors & Analytics LISA+, Universität Tübingen, Tübingen, Germany
5. Institut für Angewandte Physik, Universität Tübingen, Tübingen, Germany